REVIEW

Review on nontraditional perspectives of synthetic aperture radar image despeckling

Prabhishek Singh[a], **Achyut Shankar**[b,†] **and Manoj Diwakar**[c,*]
[a]Bennett University, School of Computer Science Engineering and Technology, Greater Noida, Uttar Pradesh, India
[b]Amity University Noida, Amity School of Engineering and Technology, Noida, Uttar Pradesh, India
[c]Graphic Era deemed to be University, Dehradun, Uttarakhand, India

Abstract. Synthetic aperture radar (SAR) image despeckling is a preprocessing method. SAR images are, by default, noisy in nature. The kind of noise found in SAR images is called speckle noise. The effect of this noise on SAR images is highly adverse. It degrades the quality of the SAR image, resulting in the loss of vital information. Since SAR images are inherently speckled in nature, it costs a lot of information loss. The removal of such noise from the SAR image is mandatory and is the first step. The elimination of speckle noise from SAR images is called SAR image despeckling. There are various traditional and nontraditional methods of SAR image despeckling based on Bayesian and non-Bayesian techniques. The SAR image despeckling methods based on Bayesian techniques are further subdivided into spatial and transform domains. This paper presents a comparative review of nontraditional perspectives on SAR image despeckling. The comparison is made based on methodology, objectives, merits, and demerits. Its focus is to do analysis of all the latest research done in the field of SAR image despeckling using nontraditional methods. © *2022 SPIE and IS&T* [DOI: 10.1117/1.JEI.32.2.021609]

Keywords: SAR image; speckle noise; nontraditional methods; Bayesian techniques; non-Bayesian techniques.

Paper 220611VSS received Jun. 15, 2022; accepted for publication Oct. 18, 2022; published online Nov. 8, 2022.

1 Introduction

A radar's antenna size determines whether it is a real aperture radar (RAR) or a synthetic aperture radar (SAR). RAR includes the noncoherent radars that are regulated by the antenna's length.[1] Active radar uses high-frequency radar waves from the antenna to deliver images to the desired area of the landscape. If the antenna's length is large, then the image captured is also big and contains a lot of Earth's surface information.[2] However, lengthening the antenna often is not a feasible solution to get high-resolution image, because on many satellites and aircraft, there is limited ability to attach large-size antennae. To get around this problem, engineers and scientists have created the synthetic aperture. When many small antennas are joined, the array of smaller antennae seems to be much bigger, allowing for better and bigger data resolution. High-resolution images of the entire Earth's surface are captured by SAR, which is a coherent radar connected to satellites and aircraft.[3] The antenna size on many satellites and aircraft is fixed in RAR, whereas in the case of SAR, the antenna mounted on satellites and aircraft is synthetic in nature, which means it moves forward and backward. As it moves forward, the SAR antenna also moves and keeps transmitting high-frequency radar waves toward the Earth's surface. These high-frequency radar waves hit the target and reflect.[4] The backscattered energy is received by the SAR and processed as well. This processing of received SAR data requires a lot of time, as it is a high computational process. The received SAR data in the form of high-resolution SAR images is resultant of consistent interaction of constructive and destructive interference of transmitted high-frequency radar waves with target on the Earth's surface.[5]

*Address all correspondence to manoj.diwakar@gmail.com

†Current affiliations: WMG, University of Warwick, Coventry, United Kingdom, and Graphic Era Deemed to be University, Department of Computer Science and Engineering, Dehradun, India

This constructive and destructive interference causes a lot of information loss as well as quality degradation during the image acquisition phase. This information loss as well as quality degradation appears in the SAR image in the form of a scattering phenomenon.[6] This scattering phenomenon is speckle noise. This speckle noise is inherently present in the SAR images. It badly degrades the image quality of SAR image.[7] The speckle noise has granular pattern that looks like the image is severely affected by salt-and-pepper noise.[8] The SAR images need to preprocess before performing any kind of classification operation on SAR images. This preprocessing is SAR image despeckling.[9] The elimination of speckle noise from SAR image is called as SAR image despeckling. This preprocessing method is a mandatory step in any kind of SAR image processing as it improves the image quality and makes further processing easier.[10] The effect of speckle noise is much bad in comparison to other kind of noise patterns.[11] Its main reason is its multiplicative nature. The pattern of speckle noise follows a gamma distribution.[12] Speckle noise is multiplicative in nature. So, it is a multiplicative noise. The effect of multiplicative noise is comparatively bad than additive noise. Here in multiplicative noise, the external noise components get multiplied by the reference SAR data resulting into noisy SAR image.[13]

There are multiple traditional and nontraditional SAR image despeckling methods. These methods are grouped into Bayesian and non-Bayesian methods. The traditional SAR image despeckling methods are mostly based on Bayesian techniques in spatial domain. While the nontraditional SAR image despeckling methods are based on Bayesian techniques in transform domain and non-Bayesian techniques. Bayesian and non-Bayesian approaches both have a few benefits and downsides. Bayesian employs probabilities of data and probabilities of both hypotheses, but non-Bayesian does not use or compute the probability of the hypothesis. Non-Bayesian approaches rely on the probabilities of seen and unobserved data and do not need the development of a prior. Bayesian approaches, on the other hand, rely on a prior and the likelihood of the observed data. There are increasing claims that Bayesian statistics is much more convenient for clinical research, as well as attempts to use both non-Bayesian and Bayesian statistics for data processing in clinical research. However, the significance of Bayesian statistics also rises, as it is fundamental for machine learning algorithms, i.e., artificial intelligence-based systems. Consequently, we should see Bayesian approaches as another potent instrument for processing our data.

Speckle noise is a serious issue in the SAR images that needs to address in the preprocessing stage. This step is considered as a mandatory step when dealing with SAR image. Because of this, a continuous advancement has been seen in this field. A lot of research has been done in multiple domains with great results as well. The traditional methods are effective in this domain but the nontraditional methods that are hybrid are more effective in this domain. The despeckling results of nontraditional methods are seen as better than the traditional methods. This paper presents a comparative analysis of many nontraditional methods for SAR image despeckling.

1.1 *Role of Wavelength in SAR Images*

Optical sensors acquire data in the visible, near-infrared, and short-wave infrared ranges of the electromagnetic spectrum (1 μm). Radar sensors use longer wavelengths, giving them unique abilities like seeing through clouds ranging from 1 cm to 1 m. It is common to refer to SAR's distinct wavelengths by letters such as X, C, P, and L. When dealing with SAR, it is crucial to keep in mind that wavelength is an important aspect to take into consideration since it impacts how the radar signal contacts with the terrain and how far a signal may penetrate a medium. In a recent letter published in Ref. 14, two novel approaches for detecting changes in SAR image stacks using the Neyman–Pearson criteria were introduced. The first suggested technique obtains background statistics from a stack of photos with different wavelength resolutions and then applies a hypothesis test to identify anomalies in a surveillance image. The second strategy considers prior knowledge of the targets to collect target data, which are then combined with background statistics to conduct a hypothesis test to spot shifts in a surveillance image. Stacks of SAR images captured at different wavelengths are analyzed statistically for clutter in the latter.[15] Images in a stack are SAR images taken with the same sensor along the same flight path, of the same location, at different times of day. This letter describes a convolutional neural network (CNN)-based incoherent change detection method (CDA) for wavelength-resolution SAR.

Fig. 1 SAR image dataset.

The proposed CDA consists of a CNN for segmentation, which localizes prospective changes, and a CNN for classification, which evaluates these candidates and classifies them as either true changes or false alarms.

1.2 *Availability of Dataset and Material*

Figure 1 shows SAR image dataset. The real SAR image dataset is taken from the open public database. The description and availability of all these images are available in the cited references. The SAR image in Fig. 1(a) belongs to Ka-band and its wavelength ranges from 1.1 to 0.8 cm available in Ref. 16. The SAR image in Fig. 1(b) belongs to C band and its wavelength ranges from 3.8 to 2.4 cm available at Ref. 17. The SAR image in Fig. 1(c) belongs to S-band and its wavelength range from 15 to 7.5 cm available at open database platform.[18,19] The SAR images in Figs. 1(d) and 1(e) are taken from the open database platform available at Ref. 20. SAR image in Fig. 1(d) belongs to same S band and SAR image in Fig. 1(e) belongs to P band and its wavelength ranges from 100 to 30 cm.

The results shown in Sec. 5.2 are evaluated and demonstrated under MATLAB environment, i.e., version: MATLAB R2022a. All the MATLAB codes are run on windows 10 pro–operating system. Processor: 11th Gen Intel(R) Core(TM), i5-1145G7 @ 2.60 GHz. Ram: 16.0 GB, Operating system type is 64-bit.

1.3 *Significance of this Study and its Major Contribution*

Most of the research done in the field of SAR image despeckling lies under two categories: Bayesian approaches in the transform domain and non-Bayesian approaches. The main methodologies that come under the Bayesian approach in the transform domain are using homomorphic and nonhomomorphic filtering. The homomorphic filtering methods are more prevalent because they can use additive restoration models easily, while nonhomomorphic filtering cannot do so. The significant filtering methods that come under non-Bayesian approaches are anisotropic diffusion, total variation, and deep learning-based methods. This paper presents how these standard methods are used in a nontraditional way. The discussed hybrid nontraditional methods show better despeckling results in terms of qualitative and quantitative analysis. The paper further discusses how traditional methods like DWT and others are incorporated with other methods like method noise thresholding and correlation-based fusion mechanisms to deliver far better results than their original results. The paper also discusses various perspectives of these nontraditional despeckling methods, like objectives, methodologies, merits, and demerits.

With the motivation of Refs. 9 and 21, this review paper focuses on comparing the most recent and best nontraditional SAR image despeckling methods that show the great despeckling result in terms of fine detail preservation without loss of any information. This paper will help and motivate the new researchers who want to work in the field of SAR image despeckling. The paper surveys only those papers that are using hybrid techniques using some prevalent mechanism. Also, it aims to compare the different papers based on their objectives, methodology, merits, and demerits.

The organization of this review paper is as follows: Sec. 1 introduces SAR image, speckle noise, SAR image despeckling, role of wavelength in SAR image, and motive of this review paper. Section 2 discusses the scattering and polarization process. Section 3 discusses the various

problems in SAR image. Section 4 discusses the latest nontraditional hybrid methods of SAR image despeckling. Section 5 compares nontraditional hybrid methods based on their objectives, merits, demerits, etc. It also analyzes few latest nontraditional hybrid methods based on their visual results and using different metrics. Last, Sec. 6 concludes the review paper.

2 Scattering and Polarization Processes

By adjusting the analyzed polarization in both transmit and receive pathways, radar may gather signals in various polarizations. The direction of oscillation of the transmitted radar signals is referred to as polarization. SAR sensors normally provide data that is linearly polarized, even though the sensors' orientation may be at any angle. The symbol H stands for horizontal polarization, whereas the letter V stands for vertical polarization. Radar sensors have the benefit of being able to accurately regulate the polarization of the sent and received signals. For signals that are both V and H polarization, they would be labeled as VH. Another way to express this is to use the abbreviation HH for H and V signals, respectively.[22]

The composition of the imaging surfaces is revealed by analyzing the signal intensity from these distinct polarizations, depending on the following scattering types: rough surface, volume, and double bounce.

- The rough surface such as bare earth or water scatters, it is the most susceptible to VV scattering.
- VH or HV cross-polarized data, such as the scattering of leaves and branches under a forest canopy, is especially susceptible to volume scattering.
- HH polarized signals are most susceptible to double bounce scattering, the last form of scattering. This is produced by structures like buildings, trees, or flooded vegetation.[23]

The different scattering types are visually shown in Fig. 2.

We must remember that various scattering types may have differing amounts of signal due to wavelength, since wavelength affects how far a signal may penetrate. As an example, a C-band signal can penetrate only the upper levels of a forest's canopy, and so will encounter predominantly roughness scattering combined with a minor degree of volume scattering. However, an L-band or P-band signal will penetrate considerably deeper and so suffer much more volume scattering and more double-bounce scattering due to the tree trunk.[24] Different SAR bands with their defined wavelength are shown in Fig. 3.

3 Problem in SAR Image

Several factors may cause the SAR system's performance to degrade and the picture quality to degrade. The nonlinearities of the SAR subsystem have a detrimental effect on the system's capacity to resolve. Image acquisition is a substantial contributor to the noise in SAR imaging

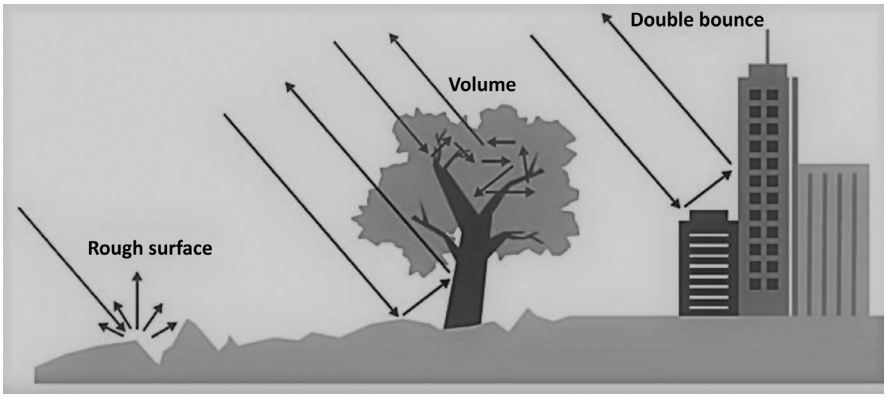

Fig. 2 Different scattering type: rough surface, volume, and double bounce.[22]

Fig. 3 SAR band: (a) X-band (3 cm); (b) C-band (6 cm); (c) L-band (24 cm); (d) P-band (65 cm).[22]

system. The sensor's location and velocity inaccuracies, which cause geometric distortion in the SAR image, are further sources of noise introduction. There are mainly four types of problems found in SAR image.[25] The major source of their introduction is briefly discussed below:

- **Geometric distortion:** Change in position of spaceborne or airborne antennae, rotation of Earth, deviation in sensor mechanism and viewing geometry, refraction and turbulence, time variations or drift and clock synchronicity.[26]
- **System nonlinear effects:** Amplitude error, phase error, quantization error, bit error noise, and system nonlinearities.[26]
- **Range migration:** Elliptical orbit and Earth rotation, target move toward the synthetic aperture, high velocities of airplanes, and satellite-borne SAR system.[27]
- **Speckle noise effects:** When high-frequency radar waves contact with target locations, the SAR image is created. Because of this ongoing contact, the image gets damaged by salt and pepper noise, which may be both constructive and destructive interactions. This granular effect is scattered across the SAR image and its adverse effects turn into speckle noise, which lowers the image quality. The SAR image has intrinsic noise in the form of a granular pattern.[28]

Speckle noise is multiplicative in nature found mainly in SAR images and medical ultrasound images. The speckle noise in SAR images follows a gamma distribution as a noise pattern. The speckle noise in medical ultrasound images follows Rayleigh distribution as a noise pattern. The shape of gamma noise is very similar to Rayleigh distribution. The main difference between these two distributions is gamma distribution starts from zero while the Rayleigh distribution does not start from zero. Figure 4 shows classical speckle pattern. The speckle noise model is represented as

$$K(g,h) = L(g,h) \times M(g,h). \tag{1}$$

In Eq. (1), speckle noise is represented as product of speckle-free pixel $L(g,h)$ to be estimated from $K(g,h)$ and multiplicative speckle noise with unit mean and standard deviation $M(g,h)$. $K(g,h)$ is the distorted pixel of the image.

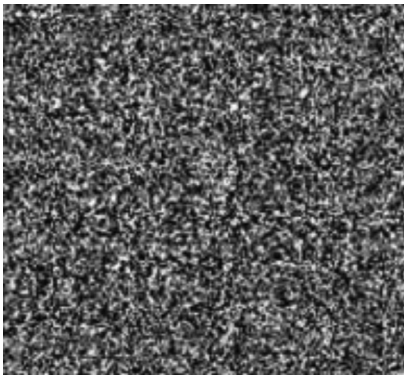

Fig. 4 Traditional speckle pattern.[9]

4 Literature Survey

Noise2noise despeckling, which can train a deep neural network using only speckled SAR images, has shown highly promising results in recent research studies. If the dataset is well-registered, then the approach employed in Ref. 29 presents a similarity estimation to adjust for the little time volatility in the data. A transformer-based network for despeckling SAR images is introduced in Ref. 30. An encoder based on a transformer enables the proposed despeckling network to learn global relationships between picture areas, which improves despeckling performance. Synthetically produced speckled images are used to train the system end-to-end. A dictionary learning and multiweighted sparse coding-based integrated SAR image despeckling model is proposed in Ref. 31. The dictionary is first trained using sets of comparable image patches, each of which has the same structural properties. For an orthogonal dictionary with good sparse representation capability, a correctly tight frame is necessary. The proposed model[31] is built using quick and efficient solution stages that conduct orthogonal dictionary learning, weight parameter updating, sparse coding and picture reconstruction concurrently. The authors in Ref. 32 provide an SAR image despeckling model based on a nonlinear hyperbolic-parabolic coupled partial differential equation (PDE). In this case, the edge variable is calculated using a different equation, resulting in improved edge information in the despeckled SAR images. The authors of Ref. 33 looked at some of the most used indicators for evaluating edge preservation. Afterward, a new reference-free index is suggested. Speckled and despeckled images use the ratio gradient to distinguish between two nonoverlapping areas on each side of each pixel. Despeckling of SAR images using a bidimensional empirical mode decomposition (BEMD)-based adaptive filtering approach is proposed by the authors of Ref. 34. SAR images with high-frequency noise are first divided into bidimensional intrinsic mode function (BIMF) levels using BEMD, and then the first BIMF level is filtered to remove the high-frequency noise. CNNs based PolSAR despeckling has been presented in Ref. 35, and it makes use of a matrix logarithm invertible transformation to make the polarimetric SAR (PolSAR) data easier to get analyzed by CNN. Speckle noise is eliminated from a damaged images by using a residual learning technique, which involves training a CNN to detect these speckles. Filtering a single-look speckled data set using the Shannon and Rényi entropies under G0 model was presented in Ref. 36.

In Ref. 37, the authors suggest a unique truncated nonconvex nonsmooth model to reduce the speckle noise in SAR pictures. Regularization and I-divergence integrity terms are also included in the formula. Despeckling performance is considerably improved by replacing a single-stream structure of convolutional layers with a multiple-stream structure to extract feature representations with multidirectional and multiscale characteristics, as shown in Ref. 38. To collect abstract aspects of an image in a certain frequency and direction band, the Contourlet CNN (CCNN) is developed with numerous separate subnetworks using the Contourlet technology. Using a combination of a deep learning network with noise reference and a similarity-based block matching, the authors of Ref. 29 have presented a new single-image speckling approach. CNNs are used in this method's denoising because they can handle tiny picture patches. Deeper CNNs have never been used previously to reduce speckle in noisy SAR pictures, according to the authors of Ref. 39. The ResNet model's many skip connections are also used in the suggested architecture of the authors. A method for applying skip connections has also been devised to ensure consistency. To train the network more consistently, a hybrid loss function was devised. A new SAR image despeckling method was developed by the authors in Ref. 40 to increase the performance of an encoder–decoder CNN architecture. The smallest scale introduces a context block to collect multiscale data. Using a blend of a revised despeckling gain and a total variation loss function, the gradient descent technique is used to train the model. In Ref. 41, a weighted sparse representation-based approach for despeckling SAR images is described. First, multiplicative noise is transformed into additive noise via the homomorphic transformation. To acquire the flexible dictionaries and sparse coefficients based on nonlocal self-similarity constraint, related patches are clustered together in a second step. Coefficients are also subjected to weighted regularizations to boost efficiency. Finally, despeckling images may be generated using an exponential transform. For SAR image despeckling, a transformer-based network was presented in Ref. 30. An encoder-based on a transformer enables the proposed method to learn global

relationships between image areas, which improves despeckling performance. Synthetically produced speckled images are used to train the system end-to-end. SSD-SAR-BS, a self-supervised deep learning approach based on Bernoulli-sampling-based self-supervised deep learning, was suggested by the authors of Ref. 42 in response to recent work on self-supervised denoising. As a result of training on actual SAR images, Bernoulli-sampled image pairs (input–target) were generated. It was after this that a network was trained on these pairings of images. To improve network performance, a dropout-based ensemble was implemented.

In Ref. 43, an improved Frost filtering technique for SAR images is presented. By employing Lee's filter coefficient, the Frost filter model incorporates an adaptively controlled decay factor for SAR images that better characterizes homogenous and edge portions of the image. With the purpose of emphasizing sound suggestions for reasonable training, the authors in Ref. 44 evaluated experimentally the influence of training set design on the effectiveness of SAR image despeckling. For SAR image despeckling,[45] presents a dilated residual shrinkage network. A main network and a shrinking subnetwork are part of the suggested technique. Convolution and residual learning are paired with soft thresholding to make up the core of the network. Within our network, we have soft thresholding and shrinking. The goal of Ref. 46 is to suggest a multi-step despeckling process: first, a CNN instructed under the fully developed speckle theory with a numerical loss function is used for despeckling; second, the speckle noise is predicted by the system for detecting the not fully developed regions where the system will generate artefacts via a statistical technique and a ratio edge detector. The authors of Ref. 47 compare the advantages and disadvantages of several training methodologies (synthetic, multitemporal, and hybrid). Three datasets were used to train four CNN-based algorithms for evaluation. Each training method has been tested on genuine SAR pictures to highlight the differences in performance between them.

To improve speckle filtering and texture preservation at the same time in SAR images, a deep encoder–decoder CNN architecture is presented in Ref. 48. The U-Net CNN has been adapted to meet this goal and has been changed and optimized in accordance with it. An algorithm for estimating speckle noise distribution and despeckled images has been reported in Ref. 49. For SAR collections in a wide range of landcover situations, this method performs well since it does not rely on any noise model. The authors of Ref. 50 developed a novel approach for despeckling SAR images that uses a deep learning engine to do nonlocal filtering. Using nonlocal filtering for SAR despeckling has shown to be quite successful. The underlying principle is to use picture self-similarity to estimate the hidden signal. It is possible to estimate the target pixel using pixel-wise nonlocal methods, which use weights based on patch-wise similarity measurements. The paper[51] provides a noisy reference-based SAR deep learning filter that uses complementary photos of the same region taken at different times as training references to solve the problem of speckle noise. Parameter-sharing CNN is used in Ref. 51 to better use the picture information. The similarity of each pixel pair across the multiple photos is also exploited to enhance the training process, which helps to decrease the training mistakes caused by changes in land-cover between different eras. The coherent imaging approach of SAR provides SAR images with intense and randomly dispersed speckle, which causes substantial interference to later applications. To cope with the impacted images,[52] suggest a network combining wavelet characteristics to despeckled the images and then assess the outcomes.

The authors of Ref. 53 came up with the image of using a recursive deep CNN model to remove speckles in SAR images. In the first place, the data-fitting and regularisation parts of the SAR variational model are split up into two separate problems: a data-fitting block and a deep CNN prior block, which are both separate problems. Finally, the gradient descent algorithm is used to solve the data-fitting block, and a predenoising residual channel attention network that uses dilation for the deep CNN prior block is used to train the network. The authors of Ref. 54 elaborate on the multilayer perceptron neural-network model for SAR image despeckling by employing a temporal series of SAR images. Unlike previous filtering approaches, this method may be taught using archival photos across an area of interest to understand the intensity features of test images and then flexibly decide the values and criteria for image despeckling by employing a neural network for image despeckling. The authors of Ref. 55 recommended using pretrained CNN models trained on additive white Gaussian noise to overcome the issue of speckle noise. The authors[55] further employed a multichannel logarithm method with Gaussian

denoising to incorporate such CNNs. It was hypothesized in Ref. 56 that SAR images may be despeckled without the need of ground truth (despeckled images). Despeckled pictures are traditionally required for training in learning-based systems. Real-world situations are frequently difficult to get the ground truth, though. To that aim, we provide a method for restoring speckled pictures only using SAR data. Several various approaches to dealing with speckle noise are examined by Ref. 57, depending on the speckle removal job and the availability of multitemporal stacks of SAR data. As an alternative to the newly announced SAR speckle removal architecture, the first approach uses a CNN model trained to eliminate additive white Gaussian noise from real images. The authors in Ref. 58 proposed a wavelet thresholding-based SAR image despeckling techniques using 2D-DWT. Here, speckled SAR image is first preprocessed using iterative inverse variance-based nonhomomorphic filter. The low-frequency components are directed to bilateral filter, and high-frequency components are directed to modified Bayesian thresholding followed by interlevel method noise thresholding. The intralevel method noise thresholding is applied as a postprocessing operation to get the final despeckled image.[58] The main motive of research[59] is the identification of image counterfeiting using illumination discrepancies. The suggested method measures the illumination qualities of various surfaces or objects inside an image. The digital forensics algorithm finds illumination disparities in an image's objects and delivers findings distinguishing between actual and false images. The objective of Ref. 60 is to construct an automated recognition model for the categorization of therapeutic plants using IoT and machine learning (ML) methods to improve the conventional medicinal system. Using Raspberry Pi 3 Model B+ (RPi) and the RPi camera, an intelligent system is presented to detect images of Indian medicinal plants in real-time and disclose their unique medicinal characteristics. The authors of Ref. 61 developed an enhanced energy-efficient fuzzy-based cognitive radio scheme for internet of things (IoT) networks based on the limits discovered in wireless communication networks. Cognitive radio-based heterogeneous wireless sensor area network, the standard technique, is compared to the suggested protocol.

5 Comparative Analysis of SAR Image Despeckling Methods

This section mainly comparatively analyzes some of most cited and prevalent nontraditional methods. It also discusses some of the standard despeckling methods as well. All the nontraditional methods discussed are latest papers from 2018 to 2022. The comparison is done based on two perspectives. First comparison is theoretical analysis that is done based on objectives, methodologies, merits, and demerits. This comparison is shown in Table 1 of Sec. 5.1. Second comparison is done based on the analysis of qualitative and quantitative results. This is done in Figs. 5 and 6, Tables 2 and 3 of Sec. 5.2. These visual results are comparatively assessed based on factors like texture and edge preservation, speckle noise suppression, artifacts generation, etc. This detailed comparison is performed on some prevalent methods.[1,3,4,29,31,34,38,39,46,54,62–67]

5.1 *Theoretical Comparative Analysis*

In this section, traditional and non-traditional despeckling methods are briefly compared on the basis of objectives, methodology, merits and demerits, which is shown in Table 1.

5.2 *Qualitative and Quantitative Comparative Analysis*

Figures 5 and 6 show the despeckling result of some of efficient latest nontraditional methods.[1,3,4,29,31,34,38,39,46,54] This comparison is made based on the visual quality of despeckling results and different metrics used for the performance analysis of these methods. The speckled SAR images taken for reference for the despeckling demonstration are shown in Figs. 1(c) and 1(d). There is no specific algorithm to do this visual quality analysis. There are certain factors/parameters based on which this comparative analysis is drawn such as no artifacts generation, edges, and image boundaries preservation, avoid over smoothing and over sharpening, visibility of low contrast objects should be maintained, texture preservation, smoothness in the homogeneous regions, and preservation of texture components in nonhomogeneous regions. Similarly,

Table 1 Comparison of traditional and nontraditional despeckling methods.

Papers	Objectives	Methodology	Merits	Demerits
2018[1]	Speckle noise reduction, edge preservation.	2D-DWT-based thresholding using directional smoothing filter and method noise thresholding	Efficiently preserves fine details, maximum information retrieval.	Computational time is high.
2020[3]	Speckle noise reduction, texture, and edge preservation.	2D-DWT-based thresholding using anisotropic diffusion and method noise thresholding	Efficiently preserves edges, maximum information retrieval, computational time is low.	In some cases, over-smoothening is observed.
2021[4]	Speckle noise reduction, maximum fine detail retrieval.	2D-DWT-based thresholding using correlation-based fusion and method noise thresholding	Efficiently preserves fine details, fusion improves final visual results.	Computational time is high.
2022[29]	Speckle noise removal and fine detail preservation.	Block-matching and noise-referenced deep learning	Application flexibility.	It could be extrapolated both by the ad hoc neural model or a pretrained one of the same sensors.
2022[31]	Speckle noise removal.	Dictionary learning and multiweighted sparse coding	Protects image texture.	In some cases, artifacts are generated.
2022[34]	Speckle noise removal.	Bidimensional empirical mode decomposition-based adaptive filtering	Restores original image component.	Execution time is high.
2021[38]	Speckle noise elimination and SAR image fine detail preservation.	Contourlet CNN	Overcompensate for the loss of gradients that results from widening the network.	Execution time is high and over-smoothening.
2021[39]	Speckle noise elimination and texture preservation.	Improved encoder–decoder CNN architecture by using various attention modules.	Captures multiscale information.	Total information of convolutional features is lost since it continues to learn representation locally.
2021[46]	Suppress noise without losing spatial details.	Statistical-based CNN algorithm.	Efficiently preserves edges.	Produces artifacts.
2019[54]	Speckle noise suppression.	Multilayer perceptron neural network.	Reduces the discrepancy between the intended and actual outputs of the neural network	Slow process.

Table 1 (*Continued*).

Papers	Objectives	Methodology	Merits	Demerits
1982[62]	Multiplicative noise is filtered digitally using an adaptive filter.	MMSE filter using locally estimated parameters values.	Execution time is less	Edges and fine details are lost.
1987[63]	Different model assumptions and a nonstationary image model are used to create adaptive restoration filters.	LLMMSE filter is used.	Efficiently eliminates speckle noise.	Loss of phase data.
1976[64]	The focus of this research is on techniques for segmenting the left ventricle from a RI-angiocardiogram. Mainly used in ultrasound medical images effecting from speckle noise.	Two techniques used: a radial scan approach and a boundary tracing methodology.	Preservation of edges and fine details. Intelligently increase in contrast between left ventricle and the background.	Computationally slow.
1980[65]	Speckle noise reduction using local image statistics. Improvement of contrast.	The noise filtering techniques are derived from the simplest version of the minimum mean-square error estimator.	Great computational economy. It can be used for parallel processing and real-time practical applications.	Fine details are disturbed in some instances.
2022[66]	Speckle noise reduction with detail recovery.	Despeckling framework composed of nonlocal blocks and detail recovery blocks.	Provides the perfect combination of despeckling and detail retention.	Not effective on real SAR images.
2022[67]	Preserve structure details, and the structure information.	SAR image despeckling based on patch wise nonlocal method using joint intensity and structure measures.	Computationally efficient.	Because of the independence criterion, gradient orientation information cannot be completely exploited.

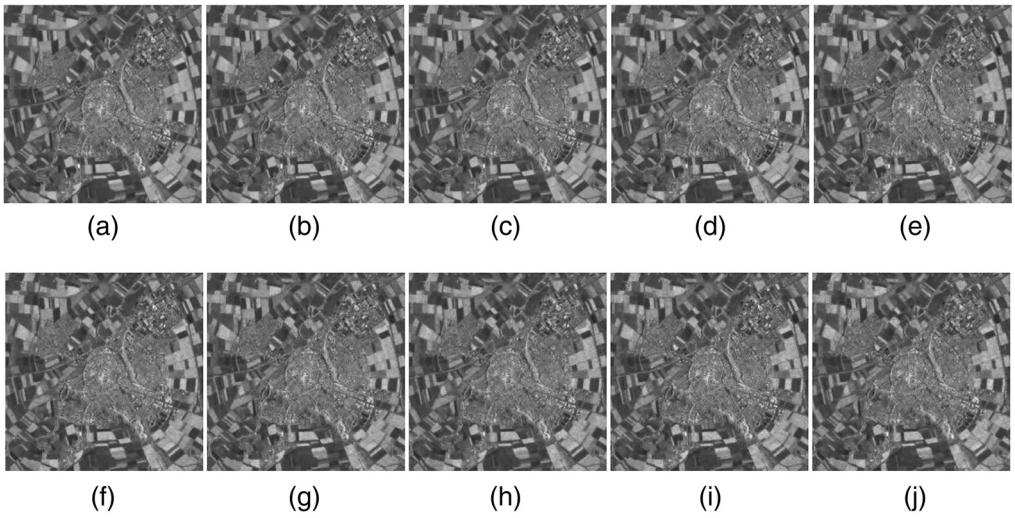

Fig. 5 Despeckling results (a) 2018,[1] (b) 2020,[3] (c) 2021,[4] (d) 2022,[29] (e) 2022,[31] (f) 2022,[34] (g) 2021,[38] (h) 2021,[39] (i) 2021,[46] and (j) 2019.[54]

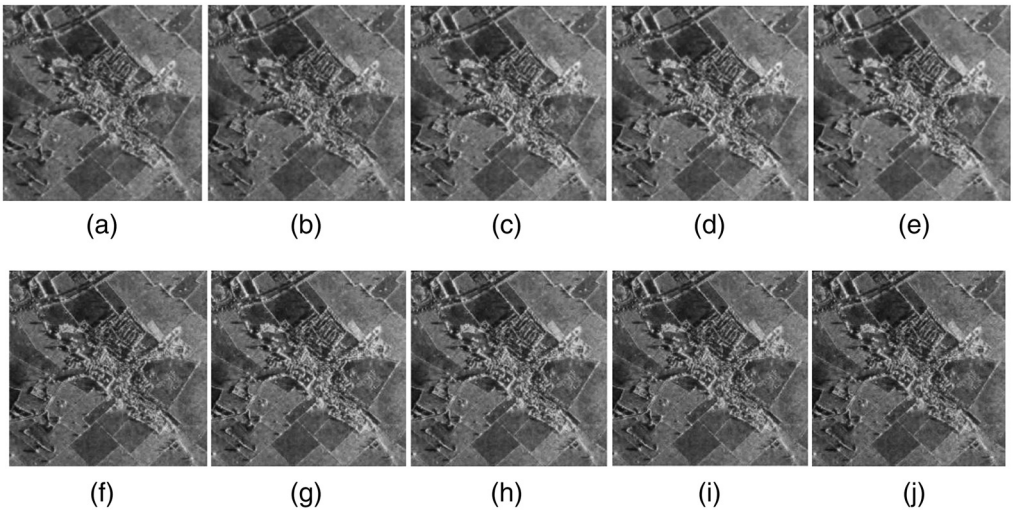

Fig. 6 Despeckling results (a) 2018,[1] (b) 2020,[3] (c) 2021,[4] (d) 2022,[29] (e) 2022,[31] (f) 2022,[34] (g) 2021,[38] (h) 2021,[39] (i) 2021,[46] and (j) 2019.[54]

the quantitative analysis is shown in Tables 2 and 3 on Figs. 1(c) and 1(d), respectively, using metrics like equivalent numbers of looks (ENL), noise variance (NV), coefficient of variation (CV), and mean-squared error (MSE). ENL analyzes the smoothness in homogeneous areas. NV tells the speckle noise content in image. CV analyzes the heterogeneous areas, and MSE determines the average difference between real speckle SAR image and speckled image. The complete description of all these metrics and its formulation are properly explained in Ref. 1.

Figure 5 compares some of the latest nontraditional despeckling methods. The reference speckled image is shown in Fig. 1(d) that is having the speckle noise variance = 0.1 (10%). All the compared methods are executed on this speckled image. The results look similar in Fig. 5 on the first look, but this difference can be better understood by zooming the image for comparative analysis. On zooming the images of Fig. 5, it is found that Figs. 5(c) and 5(e) show the best despeckling results based on edge preservation and details clarity. The despeckling results of Figs. 5(g)–5(j) are comparatively weaker in comparison to other compared methods, as blurring can be observed in Figs. 5(g) and 5(i), small edges distortion can be seen in Figs. 5(h) and 5(j). Also, noise variance looks higher even after despeckling process, as distortion is clearly

Table 2 Comparative despeckling analysis based on NV, MSE, ENL, and CV on Fig. 1(c).

Methods	NV [Fig. 1(c)]	MSE [Fig. 1(c)]	ENL [Fig. 1(c)]	CV [Fig. 1(c)]
Real speckled SAR image [Fig. 1(c)]	8.2946	—	2.0359	35.2937
1	2.9895	965.2654	2.6359	36.6254
3	2.3591	953.2314	2.8547	36.5142
4	1.3590	1068.1122	3.0213	36.3261
29	5.0271	759.3695	2.2345	37.6523
31	2.2613	1095.3265	3.1021	36.2135
34	4.6289	814.2315	2.2258	37.2514
38	3.9691	875.2643	2.3654	36.0002
39	6.4561	689.3279	2.0058	38.6352
46	6.5252	714.3262	2.1254	38.3251
54	6.0001	755.3269	2.0145	37.1210

Table 3 Comparative despeckling analysis based on NV, MSE, ENL, and CV in Fig. 1(d).

Methods	NV [Fig. 1(d)]	MSE [Fig. 1(d)]	ENL [Fig. 1(d)]	CV [Fig. 1(d)]
Real speckled SAR image [Fig. 1(d)]	7.9826	—	1.9568	34.5671
1	2.3968	913.2654	2.5625	35.5123
3	2.0059	936.5621	2.7515	35.4512
4	1.2580	1002.5565	2.9564	35.2547
29	4.8976	755.3912	2.1254	36.5140
31	1.9782	1029.3265	3.0021	35.1594
34	4.5897	798.3251	2.1189	36.1248
38	3.8978	851.2972	2.2658	35.9054
39	6.2678	680.3966	1.9965	37.5621
46	6.0258	700.2531	2.0321	37.2651
54	5.9867	725.6589	2.0096	37.0025

visible in the results. Some texture components are also lost in Figs. 5(i) and 5(j). The visual quality of Figs. 5(a) and 5(b) are also satisfactory as speckle noise is reduced and fine details are preserved. The fine details are well preserved in these cases. The despeckling results of Figs. 5(d) and 5(f) are also satisfactory in terms of smoothness and no artifact generation. The noise suppression is performed well, and fine details are also well preserved.

The result of compared despeckling methods looks quite similar in Fig. 6 as well. On zooming the images of Fig. 6, it is found that Figs. 6(c) and 6(e) show the best despeckling results in terms of preserving smoothness and edge preservation in nonuniform areas. The despeckling results of Figs. 6(g)–6(j) are comparatively weaker in comparison to other compared methods in terms of texture preservation in heterogeneous areas. The speckle noise reduction is comparatively weaker than other methods, as degradation of fine details is clearly visible in visual results.

Some edges are lost in Figs. 6(i) and 6(j) after despeckling. The overall appearance of Figs. 6(a) and 6(b) are satisfactory as speckle noise is sufficiently reduced and edge components are well preserved. The fine details are well preserved in both uniform and nonuniform regions. The despeckling results of Figs. 6(d) and 6(f) are also satisfactory in terms of noise suppression and fine texture preservation in nonhomogeneous areas.

Tables 2 and 3 compares the latest nontraditional methods[1,3,4,29,31,34,38,39,46,54] using different metrics, i.e., NV, MSE, ENL, CV on Figs. 1(c) and 1(d), respectively. In Table 2, NV (4) = 1.3591 that represents the best result in terms of noise reduction. NV (46) = 6.5252 that represents the comparative least optimal result in terms of noise reduction. The NV of real speckled SAR image Fig. 1(c) = 8.2946. Based on NV values of,[1,3,31] it can be easily said that speckle reduction is well performed by these methods. The methods[31,34,38] shows satisfactory result in terms of speckle reduction. Based on MSE values in Table 2, it can be said that[4,31] has higher MSE values that show the significant difference between speckled and despeckled image results. It represents effective despeckling process. The MSE values of Refs. 29, 39, 46, and 54 are lesser in comparison to other methods value. These methods show weak despeckling process. The despeckling results of Refs. 1, 3, and 38 are better as they yield better MSE values. The CV value of speckled image is 35.2937. When the CV value of despeckled image is less than CV value of speckled image, it represents poor preservation of fine details. When the CV value of despeckled image is more than CV value of speckled image, it represents the introduction of impairments. The CV of all compared methods is higher than CV of Fig. 1(c), this means details are quite well preserved by these methods. But the increasing difference of CV is significant in case of Refs. 29, 34, 46, and 54, therefore, in these method results, impairments can be observed. Rest other method results are considered as best. Based on ENL values, it can be easily said that[3,4,31] presents the best results due to higher values. Rest of other method ENL values are satisfactory.

In Table 3, quantitative analysis of despeckling methods in Fig. 1(d) is presented. The NV of real speckled image is 7.9826. The methods that show the best performance based on NV values are.[4,31] After that, methods like[1,3] also show great results. The results of[29,34,38] are also satisfactory. While rest of the methods shows below satisfactory results. Based on the MSE values,[4,31] shows best performance. The methods[1,3] also show great results, as good speckle content removal can be observed.[38] also shows satisfactory results. While the rest of the methods shows below satisfactory results based on MSE values. Based on ENL values,[31] show the best results, and show least best results.[39] While rest of the methods shows almost similar results. The CV of speckled image is 34.5671. The CV values of all despeckling methods are greater than the CV value of reference speckled image, but this increasing difference is not significant in Refs. 1, 3, 4, 31, and 38 so there is no introduction of impairments in the results. This increasing difference of CV value is significant in the case of Refs. 39, 46, and 54, so here on zooming the output images, some impairments can be observed. While rest of the methods shows satisfactory result because of average difference of CV values.

The despeckling result evaluation of[1,3,4,29,31,34,38,39,46,54] on the dataset (Fig. 1) was complex task. There are various efficient nontraditional despeckling methods available in the present literature. Out of them, finding out such nontraditional despeckling methods that are efficient and that can be implemented on the dataset (Fig. 1) was not that easy. The results evaluation of all the selected nontraditional despeckling methods is done on real speckled SAR images, which requires no hypothesis. Such methods are taken into consideration that can be compared using similar metrics as presented in Tables 2 and 3. Such methods are taken into consideration that can be compared based on naked eye visual analysis using certain factors discussed in subsection of qualitative analysis. The nontraditional despeckling methods are similar in terms of their major objectives, which is the elimination of speckle noise while preserving the fine details. The main limitation of Ref. 1 is its high computational time. The main limitation of Ref. 3 is over-smoothening. The main limitation of Ref. 4 is its high computational time. The main limitation of Ref. 29 is that it could be extrapolated both by the ad hoc neural model or a pretrained one of the same sensors. The main limitation of Ref. 31 is that somewhere in the despeckling process, the artifacts are generated. The main limitation of Ref. 34 is its high execution time. The main limitation of Ref. 38 is its high execution time and over-smoothening. The main limitation of Ref. 39 is that the total information on convolutional features is lost. The main limitation of

Ref. 46 is that it produces artifacts during the process, and the main limitation of Ref. 54 is its slowness.

6 Conclusion

This review surveys various nonconventional SAR image despeckling methods and a few traditional methods as well. It further discusses the basics of SAR imaging, including scattering and polarization effects, and problems present in SAR imaging. The compared methods range from the year 2018 to 2022. A more specific comparative analysis has been done of some of the major despeckling works in recent years. This comparison is done using theoretical analysis, qualitative analysis, and quantitative analysis. The theoretical analysis is done based on the objectives set, methods used, and merits and demerits of these papers. The qualitative analysis is done based on a certain set of factors that are discussed in the related section. The quantitative analysis is performed using parameters like NV, ENL, MSE, and CV. The analysis is done in detail by explaining all its perspectives. The survey performed on these methods mostly uses hybrid methodology. This will help the researchers to understand the standard methods used in the discussed papers and they will get an idea of how to design approaches for SAR image despeckling methods.

References

1. P. Singh and R. Shree, "A new SAR image despeckling using directional smoothing filter and method noise thresholding," *Eng. Sci. Technol. Int. J.* **21**(4), 589–610 (2018).
2. P. Singh and R. Shree, "Analysis and effects of speckle noise in SAR images," in *2nd Int. Conf. Adv. Computing, Commun., & Autom. (ICACCA)*, Fall, September, IEEE, pp. 1–5 (2016).
3. P. Singh and R. Shree, "A new homomorphic and method noise thresholding based despeckling of SAR image using anisotropic diffusion," *J. King Saud Univ.-Comput. Inf. Sci.* **32**(1), 137–148 (2020).
4. P. Singh, R. Shree, and M. Diwakar, "A new SAR image despeckling using correlation-based fusion and method noise thresholding," *J. King Saud Univ.-Comput. Inf. Sci.* **33**(3), 313–328 (2021).
5. P. Singh and R. Shree, "Quantitative dual nature analysis of mean square error in SAR image despeckling," *Int. J. Comput. Sci. Eng.* **9**(11), 619–622 (2017).
6. P. Singh and R. Shree, "A new computationally improved homomorphic despeckling technique of SAR images," *Int. J. Adv. Res. Comput. Sci.* **8**(3), 589–610 (2017).
7. P. Singh and R. Shree, "Statistical quality analysis of wavelet based sar images in despeckling process," *Asian J. Electr. Sci.* **6**(2), 1–18 (2017).
8. P. Singh and R. Shree, "Statistical modelling of log transformed speckled image," *Int. J. Comput. Sci. Inf. Security* **14**(8), 426 (2016).
9. P. Singh et al., "A review on SAR image and its despeckling," *Arch. Comput. Methods Eng.* **28**(7), 4633–4653 (2021).
10. P. Singh and R. Shree, "Speckle noise: modelling and implementation," *Int. J. Control Theor. Appl.* **9**(17), 8717–8727 (2016).
11. P. Singh and R. Shree, "Importance of DWT in despeckling SAR images and experimentally analyzing the wavelet based thresholding techniques," *Int. J. Eng. Sci. Res. Technol.* **5**(10), 894–898 (2016).
12. P. Singh and R. Shree, "Impact of method noise on SAR image despeckling," *Int. J. Inf. Technol. Web Eng.* **15**(1), 52–63 (2020).
13. R. Shree et al., "A critical review on despeckling methods in agricultural SAR image," *Int. J. Appl. Exercise Physiol.* **9**(7), 258–266 (2020).
14. D. I. Alves et al., "Neyman–Pearson criterion-based change detection methods for wavelength–resolution SAR image stacks," *IEEE Geosci. Remote Sens. Lett.* **19**, 1–5 (2022).
15. D. I. Alves et al., "A statistical analysis for wavelength-resolution SAR image stacks," *IEEE Geosci. Remote Sens. Lett.* **17**(2), 227–231 (2020).

16. SAR Image Datase, 2021, https://www.sandia.gov/radar/pathfinder-radar-isr-and-synthetic-aperture-radar-sar-systems/archive-imagery/ (accessed January 2022).
17. PIA01763: Space Radar Image of Kilauea, Hawaii – Interferometry 1, 1999, https://photojournal.jpl.nasa.gov/catalog/PIA01763 (accessed January 2022).
18. "Dataset of standard [512 × 512] Grayscale test images," 2010, https://decsai.ugr.es/ (accessed January 2022).
19. SAR Test Images, 2005, https://ccia.ugr.es/cvg/dbimagenes/ (accessed January 2022).
20. SAR Test Images, 2008, https://eo.belspo.be/en (accessed January 2022).
21. F. Argenti et al., "A tutorial on speckle reduction in synthetic aperture radar images," *IEEE Geosci. Remote Sens. Mag.* **1**(3), 6–35 (2013).
22. "What is synthetic aperture radar?," 2010, https://www.earthdata.nasa.gov/learn/backgrounders (accessed January 2022).
23. "RADAR vs OPTICAL earth observation – why both?," 1997, http://sar.ece.ubc.ca/SARintro/SAR.html#:~:text=SAR%20uses%20a%20wavelength%20of,while%20optical%20sensors%20can%20not (accessed January 2022).
24. "Difference between SAR image and optical image | SAR vs. optical sensors," https://www.gofastresearch.com/2022/02/difference-between-sar-image-and.html (accessed 07 June 2022).
25. M. S. Ranga Rao and P. R. Mahaptra, "Synthetic aperture radar: a focus on current problems," *Defence Sci. J.* **47**(4), 517–536 (1997).
26. T. Toutin, "Review article: geometric processing of remote sensing images: models, algorithms and methods," *Int. J. Remote Sens.* **25**(10), 1893–1924 (2004).
27. A. L. Choo, Y. K. Chan, and V. C. Koo, "Geometric correction on SAR imagery," in *Progr. Electromagn. Res. Symp. Proc.*, 27–30 March, KL, Malaysia (2012).
28. A. Moreira et al., "A tutorial on synthetic aperture radar," *IEEE Geosci. Remote Sens. Mag.* **1**(1), 6–43 (2013).
29. C. Wang et al., "SAR image despeckling based on block-matching and noise-referenced deep learning method," *Remote Sens.* **14**(4), 931 (2022).
30. M. V. Perera et al., "Transformer-based SAR image despeckling," arXiv:2201.09355 (2022).
31. S. Liu et al., "Synthetic aperture radar image despeckling based on multi-weighted sparse coding," *Entropy* **24**(1), 96 (2022).
32. S. Majee, R. K. Ray, and A. K. Majee, "A new non-linear hyperbolic-parabolic coupled PDE model for image despeckling," *IEEE Trans. Image Process.* **32**, 1963–1977 (2022).
33. X. Ma, H. Hu, and P. Wu, "A no-reference edge-preservation assessment index for SAR image filters under a Bayesian framework based on the ratio gradient," *Remote Sens.* **14**(4), 856 (2022).
34. R. K. Painam and M. Suchetha, "Despeckling of SAR images using BEMD-based adaptive frost filter," *J. Indian Soc. Remote Sens.* **50**, 1–12 (2022).
35. D. Tucker and L. C. Potter, "Polarimetric SAR despeckling with convolutional neural networks," *IEEE Trans. Geosci. Remote Sens.* **60**, 1–12 (2022).
36. D. Chan, J. Gambini, and A. C. Frery, "Entropy-based non-local means filter for single-look SAR speckle reduction," *Remote Sens.* **14**(3), 509 (2022).
37. M. Guo et al., "A novel truncated nonconvex nonsmooth variational method for SAR image despeckling," *Remote Sens. Lett.* **12**(2), 122–131 (2021).
38. G. Liu et al., "Contourlet-CNN for SAR image despeckling," *Remote Sens.* **13**(4), 764 (2021).
39. A. Passah, K. Amitab, and D. Kandar, "SAR image despeckling using deep CNN," *IET Image Process.* **15**(6), 1285–1297 (2021).
40. J. Ko and S. Lee, "SAR image despeckling using continuous attention module," *IEEE J. Sel. Top. Appl. Earth Observ. Remote Sens.* **15**, 3–19 (2022).
41. J. Zhang et al., "Learning an SAR image despeckling model via weighted sparse representation," *IEEE J. Sel. Top. Appl. Earth Observ. Remote Sens.* **14**, 7148–7158 (2021).
42. Y. Yuan et al., "An advanced SAR image despeckling method by Bernoulli-sampling-based self-supervised deep learning," *Remote Sens.* **13**(18), 3636 (2021).
43. Y. Pan, Y. Meng, and L. Zhu, "SAR image despeckling method based on improved Frost filtering," *Signal Image Video Process.* **15**(4), 843–850 (2021).

44. A. Mazza et al., "Impact of training set design in CNN-based SAR image despeckling," in *IEEE Int. Geosci. Remote Sens. Symp. IGARSS*, July, IEEE, pp. 415–418 (2021).
45. N. Lin et al., "Dilated residual shrinkage network for SAR image despeckling," in IEEE *6th Int. Conf. Signal and Image Process. (ICSIP)*, October, IEEE, pp. 503–507 (2021).
46. S. Vitalea, G. Ferraiolib, and V. Pascazio, "Statistical based CNN algorithm for SAR image despeckling," in *EUSAR 13th Eur. Conf. Synthetic Aperture Radar*, March, VDE, pp. 1–5 (2021).
47. S. Vitale, G. Ferraioli, and V. Pascazio, "Analysis on the building of training dataset for deep learning sar despeckling," *IEEE Geosci. Remote Sens. Lett.* **19**, 1–5 (2022).
48. F. Lattari et al., "Deep learning for SAR image despeckling," *Remote Sens.* **11**(13), 1532 (2019).
49. A. G. Mullissa et al., "DeSpeckNet: generalizing deep learning-based SAR image despeckling," *IEEE Trans. Geosci. Remote Sens.* **60**, 1–15 (2022).
50. D. Cozzolino et al., "Nonlocal CNN SAR image despeckling," *Remote Sens.* **12**(6), 1006 (2020).
51. X. Ma et al., "SAR image despeckling by noisy reference-based deep learning method," *IEEE Trans. Geosci. Remote Sens.* **58**(12), 8807–8818 (2020).
52. J. Zhang, W. Li, and Y. Li, "SAR image despeckling using multiconnection network incorporating wavelet features," *IEEE Geosci. Remote Sens. Lett.* **17**(8), 1363–1367 (2020).
53. H. Shen et al., "SAR image despeckling employing a recursive deep CNN prior," *IEEE Trans. Geosci. Remote Sens.* **59**(1), 273–286 (2021).
54. X. Tang, L. Zhang, and X. Ding, "SAR image despeckling with a multilayer perceptron neural network," *Int. J. Digit. Earth* **12**(3), 354–374 (2019).
55. X. Yang et al., "SAR image despeckling using pre-trained convolutional neural network models," in *Joint Urban Remote Sens. Event (JURSE)*, May, IEEE, pp. 1–4 (2019).
56. K. Ravani, S. Saboo, and J. S. Bhatt, "A practical approach for SAR image despeckling using deep learning," in *IGARSS 2019-2019 IEEE Int. Geosci. and Remote Sens. Symp.*, July, IEEE, pp. 2957–2960 (2019).
57. E. Dalsasso et al., "SAR image despeckling by deep neural networks: from a pre-trained model to an end-to-end training strategy," *Remote Sens.* **12**(16), 2636 (2020).
58. P. Singh et al., "MSPB: intelligent SAR despeckling using wavelet thresholding and bilateral filter for big visual radar data restoration and provisioning quality of experience in real-time remote sensing," *Environ. Dev. Sustain.* **9**, 1–31 (2022).
59. M. Kumar and S. Srivastava, "Identifying photo forgery using lighting elements," *Indian J. Sci. Technol.* **9**(48), 1–5 (2016).
60. R. Shailendra et al., "An IoT and machine learning based intelligent system for the classification of therapeutic plants," *Neural Process. Lett.* **54**, 4465–4493 (2022).
61. P. Chithaluru et al., "An enhanced energy-efficient fuzzy-based cognitive radio scheme for IoT," *Neural Comput. Appl.* **34**, 1–23 (2022).
62. V. S. Frost et al, "A model for radar images and its application to adaptive digital filtering of multiplicative noise," *IEEE Trans. Pattern Anal. Machine Intell.* **PAMI-4**, 157–166 (1982).
63. D. T. Kuan et al., "Adaptive restoration of images with speckle," *IEEE Trans. Acc. Speech Signal Proc.* **35**(3), 373–383 (1987).
64. M. Kuwahara et al., "Processing of RI-angiocardiographic images," in *Digital Processing of Biomedical Images*, K. Preston, Jr. and M. Onoe, Eds., pp. 187–202, Plenum, New York (2022).
65. J. S. Lee, "Digital image enhancement and noise filtering by use of local statistics," *IEEE Trans. Pattern Anal. Mach. Intell.* **PAMI-2**(2), 165–168 (1980).
66. W. Wu et al., "SAR-DRDNet: a SAR image despeckling network with detail recovery," *Neurocomputing* **493**, 253–267 (2022).
67. D. Liang, M. Jiang, and J. Ding, "Fast patchwise nonlocal SAR image despeckling using joint intensity and structure measures," *IEEE J. Sel. Top. Appl. Earth Observ. Remote Sens.* **15**, 6283–6293 (2022).

Prabhishek Singh received his PhD, MTech, and BTech degrees in the field of CSE. He is working as an assistant professor in the School of Computer Science Engineering and Technology, Bennett University (Times of India Group), Greater Noida, India. He has published more than 100 research papers in SCI/SCIE/Scopus, ESCI journals, and conferences. He is serving as an associate editor, academic editor, review editor, guest editor, and editorial committee chair of many SCI/SCIE/Scopus and ESCI journals.

Achyut Shankar received his PhD in CSE from VIT University, Vellore, India. He is an assistant professor at Amity University, India. He has published more than 100 research papers in reputed international conferences and journals in which 65 papers are in SCIE journals. He is currently serving as an associate editor or guest editor in many Scopus, ESCI and World Scientific journals. He is a member of ACM and has received research award for excellence in research.

Manoj Diwakar is currently working as an associate professor in the CSE Department at Graphic Era University, Dehradun. With 10 years of industrial and academic experience, he is committed and dedicated to continuous uplift of the research environment in the department. He has published more than 100 research papers in SCI/SCIE/Scopus, ESCI journals, and conferences. He is serving as an associate editor, academic editor, review editor, guest editor, and editorial committee chair of many SCI/SCIE/Scopus and ESCI journals.